Design and experiment of the crushing roller equipped with straight and L-shaped combined blades for straw incorporation

Jie Liu[1], Senpeng Zhan[1], Yujing Yang[1], Xin Shu[1], Fang Liang[1,2*]

(1. *College of Engineering, Huazhong Agricultural University, Wuhan 430070, China*;
2. *Key Laboratory of Agricultural Equipment in Mid-lower Yangtze River, Ministry of Agriculture and Rural Affairs, Wuhan 430070, China*)

Abstract: In order to improve the crushing efficiency and spreading uniformity of rice straw incorporation, considering its characteristics of high stubble, dense structure, and strong toughness, a rice straw incorporation machine by crushing-rotary tillage-burying with a crushing roller equipped with straight blades and L-shaped blades was designed. This design leveraged the crushing and kneading action of the straight blades and the cutting and crushing effect of L-shaped blades. With the qualification rate of crushing straw and straw spreading uniformity as evaluation indicators, a mixed-level orthogonal experiment (four levels for two factors and two levels for two factors) was conducted to analyze the effects of radial angle, L-shaped blade bending angle, rotational speed, and forward speed on the qualification rate of crushing straw and straw spreading uniformity. The results showed that the factors affecting the qualification rate of crushing straw, in descending order of significance, were radial angle, rotational speed, and L-shaped blade bending angle. Those affecting straw spreading uniformity, in the same order of significance evaluation, were radial angle, L-shaped blade bending angle, forward speed, and rotational speed. The optimal parameter combination was determined as a radial angle of 70°, an L-shaped blade bending angle of 135°, a rotational speed of 2400 r/min, and a forward speed of 0.60 m/s. The experiment was conducted using the optimal parameter combination, the qualification rate of crushing straw reached 92.41%, and the straw spreading uniformity was 87.44%. Compared with the best-performing experimental group, the qualification rate of crushing straw increased by 1.86 percentage points, while the straw spreading uniformity was only 0.75 percentage points lower than the maximum value. Compared to China's national standard requirements, the optimized results show a 2.41 percentage point increase in straw crushing qualification rate and a 12.44 percentage point increase in straw spreading uniformity, thus meeting and exceeding China's national standards. The qualification rate of straw crushing and the uniformity of straw spreading were better than other combined blades. This study provides both theoretical and technical support for reducing the adverse effects of rice straw incorporation on subsequent crops.

Keywords: straw incorporation, crushing roller, parameter optimization, field experiment
DOI: 10.25165/j.ijabe.20261901.10023

Citation: Liu J, Zhan S P, Yang Y J, Shu X, Liang F. Design and experiment of the crushing roller equipped with straight and L-shaped combined blades for straw incorporation. Int J Agric & Biol Eng, 2026; 19(1): 88–96.

1 Introduction

According to data released in the China Statistical Yearbook 2024, the total sown area of rice in China was 28.95 million hm^2 in 2023. Based on this, the estimated quantity of rice straw was approximately 208 Mt. Specifically, rice planting area accounts for a quarter of the country's crop planting area, and the quantity of rice straw accounts for a quarter of the country's total straw[1,2]. Mechanized straw incorporation has become the primary method for straw resource utilization due to its advantages of being pollution-free, recyclable, and low-cost[3,4]. However, with the promotion and application of crop densification for increased yields and semi-feed low-loss harvesting (which only harvests the rice panicles), the amount of straw left in the fields increased, and the volume of straw incorporation grew year by year, exerting an increasingly significant impact on the germination and growth of subsequent crops. Sun et al. found that grain yields in long-term straw incorporation fields were 3.5% lower than in fields without straw incorporation[5]. Similarly, Wang et al.[6] demonstrated through controlled experiments that straw incorporation reduced rice yields by 0.9% to 11.8% compared with straw removal. This has led to growing skepticism about straw incorporation, and calls for the resumption of straw burning have become increasingly vocal[7,8]. There is an urgent need to improve the quality of straw incorporation and reduce its adverse effects.

Research indicated that reducing the length of straw crushing and improving the uniformity of straw distribution on the soil surface and in the soil could accelerate straw decomposition and promote seedling emergence and growth of subsequent crops. Latifmanesh et al.[9] found that increasing the proportion of straw mass in the 0-10 cm layer during straw incorporation could facilitate straw decomposition. Negiş et al.[10] found through controlled experiments that uniformly burying corn straw in the soil facilitated faster decomposition, increased soil nutrients, and improved crop yields. Yang[11] found that rapeseed straw with a length ≤10 cm decomposes much faster than rapeseed straw with a length >10 cm. Pang[12] found that corn straw with a crushed length

Received date: 2025-07-14 **Accepted date:** 2026-01-20
Biographies: Jie Liu, MS candidate, research interest: mechanical engineering, Email: 1284791490@qq.com; **Senpeng Zhan**, MS candidate, research interest: mechanical engineering, Email: 2805281319@qq.com; **Yujing Yang**, Undergraduate, research interest: mechanical and electronic engineering, Email: 862146580@qq.com; **Xin Shu**, MS candidate, research interest: agricultural mechanization engineering, Email: 2671715727@qq.com.
***Corresponding author: Fang Liang**, PhD, Associate Professor, research interest: mechanism and application of soil-machine-crop interaction. College of Engineering, Huazhong Agricultural University, Wuhan 430070, China. Tel: +86-18771938723. Email: lf@mail.hzau.edu.cn.

of 3-5 cm has a higher decomposition rate than corn straw with a crushed length of 5-10 cm. Hu et al.[13] found that the decomposition rate of rice straw was faster at a burial depth of 5 cm than at 10 cm or on the soil surface. Qin et al.[14] found that maintaining uniform crushing and spreading during straw incorporation could achieve full straw incorporation while providing a good no-till planting environment. Tian et al.[15] conducted micro-area experiments on uneven straw incorporation of wheat straw. The results showed that localized straw accumulation led to excessive accumulation of reducing substances, severely affecting rice seedling emergence and establishment, and also had a certain impact on the early growth of rice seedlings. The research team found that when the coefficient of variation in the mass distribution of rapeseed straw buried to the field was 0 (i.e., completely uniform distribution), the germination rate and plant height of maize were higher. The shorter the crushed straw length was, the more significant positive effect it exerted on the seedling emergence rate of maize, which was specifically manifested in that for every 1 cm reduction in straw length, the seedling emergence rate increased by 3.83%. In addition, for every 1 cm reduction in straw length, the plant height increased by 1.32 cm[16].

In order to improve the degree of straw crushing and the uniformity of spreading, straw crushing methods have evolved from direct crushing (horizontal crushing) to pick-up crushing, multi-stage crushing (two-axle crushing), and pick-up crushing with distribution, continuously enhancing the qualification rate of straw crushing and the uniformity of straw spreading. Shi et al.[17] designed an equipment for straw crushing with strip-laying and seed-belt classification with cleaning under full straw incorporation, adopting a pickup-crushing process, achieving a straw crushing qualification rate of 91.25%; Sun et al.[18] designed a differential sawing rice straw chopper for straw incorporation which achieved a straw crushing qualification rate of 93.23% and a straw spreading uniformity of 79.11% after optimization and experimental verification. Liu et al.[19] designed an active centrifugal rice straw spreading device for a rice combine harvester, with a coefficient of variation for lateral spreading uniformity of 17.34%. Lin et al.[20] designed a variable-speed straw crushing incorporation machine based on PLC control with equal diameter cam transmission, with a straw crushing qualification rate of 92.17%. Yan et al.[21] designed a side-throwing cotton stalk crushing incorporation device, where the spreading device adopted a spreading leaf structure, achieving an average straw spreading uniformity of 86.98%. Ergashev et al.[22] designed a rice straw incorporation machine, which could ensure that 96% of the straw is crushed and spread under optimal parameters. Chebotaryev et al.[23] designed a towed straw crushing incorporation machine, with crushing roller and spiral spreading devices at the front and rear ends of the frame, enabling effective straw crushing and uniform straw spreading.

The crushing roller is a key component of the straw crushing incorporation machine, and its structure and parameters play a crucial role in improving crushing efficiency and spreading uniformity. Commonly used crushing blades include hammer claw-type crushing blades and swing-type crushing blades (straight blades, L-shaped blades, and Y-shaped blades)[24-26]. Some scholars have also designed new crushing blades based on existing research. For example, Jia et al.[27] designed a V-L shaped blade, which improved the stability of the blades during the rotation of the crushing roller. Zhang et al.[28] designed a bionic blade for a banana straw crushing and spreading machine, inspired by the teeth of a blue shark, which required significantly less force to cut straw compared to a straight blade with a smooth edge. Luo et al.[29] designed a wheat seeder with an inter-row mulching and straw crushing function for full-straw and hard stubble fields, which adopted combined blades and added straight blades between the Y-shaped blades, exhibiting excellent pickup and crushing capabilities. Field experiments showed that the average crushed straw length was 11 cm, and the qualification rate of straw crushing reached 91.47%. Zhang et al.[30] designed a straw crushing incorporation machine, adopting a combination of cross-shaped straight blades and L-shaped blades. The qualification rate of straw crushing reached 90.01%, whereas the uniformity of straw spreading achieved 77.05%. Farm Power and Machinery developed a towed rice straw crushing incorporation machine with a combination of two L-shaped blades into one Y-shaped blade, with a straw crushing qualification rate of up to 89.8%[31]. The combination of blades was conducive to improving the degree of straw crushing.

Considering the characteristics of rice straw, including high stubble height, high density, and strong toughness, this study designed a rice straw incorporation machine by crushing-rotary tillage-burying. The machine adopts a crushing-rotary tillage-burying process and optimizes the crushing roller equipped with straight and L-shaped combined blades for straw incorporation, to improve the degree of straw crushing and the uniformity of straw spreading, thereby providing technical and theoretical support for mitigating the adverse effects of rice straw incorporation on subsequent crops.

2 Structure and working principle

2.1 Structure and working principle of rice straw incorporation machine by crushing-rotary tillage-burying

The structure and working principle of the rice straw incorporation machine by crushing-rotary tillage-burying are shown in Figure 1. It is primarily composed of a crushing roller with straight and L-shaped combined blades, a rotary tillage roller, a burying roller, an intermediate gearbox, a crushing roller gearbox, a burying roller gearbox, two drive shafts, a frame, and a three-point suspension device. Power from the tractor's rear output shaft is transmitted to the input shaft of the intermediate gearbox via a universal joint. The intermediate gearbox is equipped with three output shafts: one central and two lateral. The central output shaft drives the rotary tillage roller, while the left and right output shafts transmit power through the crushing roller drive shaft and the burying roller drive shaft to the crushing roller transmission and the burying roller gearbox, respectively. After gear adjustment, these transmissions drive the crushing roller and the burying roller.

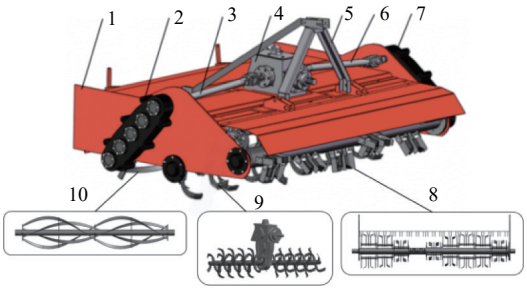

1. Frame 2. Burying roller gearbox 3. Burying roller drive shaft 4. Intermediate gearbox 5. Three-point suspension 6. Crushing roller drive shaft 7. Crushing roller gearbox 8. Crushing roller 9. Rotary tillage roller 10. Burying roller

Figure 1 Structure of rice straw incorporation machine by crushing-rotary tillage-burying

The overall operating principle of the machine is illustrated in Figure 2. During operation, the crushing roller crushes the rice straw and spreads it across the soil surface. The rotary tillage roller completes the cultivation of the soil and the secondary crushing of the straw, incorporating the straw into the soil. The burying roller adopts two spiral belts of different diameters rotating in opposite directions to achieve bidirectional axial and vertical movement of the straw and soil, thereby mixing them thoroughly.

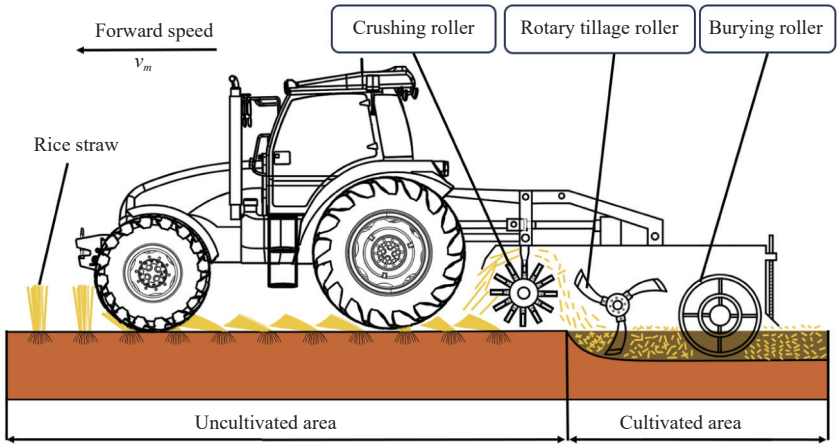

Figure 2 Schematic diagram of working principle of rice straw incorporation machine by crushing-rotary tillage-burying

2.2 Structure of crushing roller

The crushing roller structure is illustrated in Figure 3, primarily consisting of combined blades, a blade shaft, a cover shell, and fixed blades. Each combined blade consists of three straight blades, two L-shaped blades (where θ is the bending angle of the L-shaped blade), cylindrical pins, four blade holders, four sleeves, and cotter pins. The cylindrical pins pass through the holes on adjacent blade holders, and the three straight blades and two L-shaped blades are secured at both ends of the blade holders with four sleeves. The cotter pins are inserted into the through holes at both ends of the cylindrical pins to achieve axial positioning of the blades along the cylindrical pin axis. The fixed blades are welded to the cover shell. During the rotation of the crushing roller, it works in conjunction with the fixed blade to cut, crush, and spread the straw.

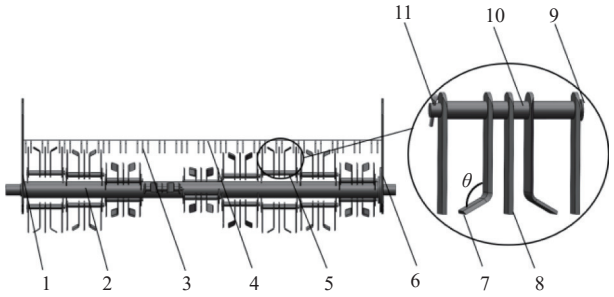

1. Left side plate 2. Blade shaft 3. Fixed blade 4. Cover shell 5. Combined blades 6. Right side plate 7. L-shaped blade 8. Straight blade 9. Cylindrical pin 10. Sleeve 11. Cotter pin

Figure 3 Structure of the crushing roller

3 Parameter design of crushing roller

The motion of the crushing roller is a combination of random linear motion and rotational motion. With the forward direction of the machine as the positive x-axis, the horizontal and vertical direction of the machine as the y-axis, and the center of rotation of the crushing roller as the origin of the coordinate system, a plane coordinate system was established, and the trajectory curve of the crushing roller blade tip is shown in Figure 4.

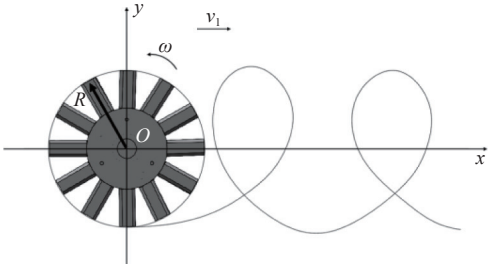

Figure 4 Motion trajectory of the blade tip point in crushing roller

The equation for the motion trajectory of the tip of the blade is:

$$\begin{cases} x = v_1 t + R\cos\omega t \\ y = R\sin\omega t \end{cases} \quad (1)$$

Differentiating Equation (1) yields the velocity of the tip point of the blade:

$$\begin{cases} v_x = v_1 - R\omega\sin\omega t \\ v_y = R\omega\cos\omega t \end{cases} \quad (2)$$

According to Equation (2), the resultant velocity of the tip point of the blade is derived as:

$$v_2 = \sqrt{v_1^2 - 2v_1 R\omega\sin t + R^2\omega^2} \quad (3)$$

When $\omega t = (4k+1)\cdot\pi/2$ (where k is a positive integer), the direction of the blade's linear velocity is opposite to the direction of the machine's forward speed. At this moment, the resultant velocity reaches its minimum value, which is equal to:

$$v_2 = R\omega - v_1 \quad (4)$$

Substituting $\omega = 2\pi n$ into Equation (4) yields the minimum value of the crushing roller speed as:

$$n = \frac{30(v_1 + v_2)}{\pi R} \quad (5)$$

In Equations (1)-(5), R is the radius of rotation of the blade tip of the crushing roller, mm; v_1 is the forward speed, m/s; ω is the angular velocity of the blade tip point of the crushing roller, rad/s; t is the duration of motion, s; v_x is the component velocity of the blade tip point along the x-axis, m/s; v_y is the component velocity of the blade tip point along the y-axis, m/s; v_2 is the resultant velocity

of the blade tip point, m/s; n is the minimum rotational speed of the crushing roller, r/min.

A larger crushing roller radius increases the machine's volume and power consumption, while a smaller radius reduces the cutting speed and affects the cutting performance of the blades. In this study, the crushing roller radius was set to 240 mm. To ensure stem crushing, the blade tip's cutting speed should be no less than 34 m/s[32], and a value of 43 m/s was adopted in this study. For a commonly applied forward speed of 1 m/s for straw-crushing incorporation machines, substituting the above parameters into Equation (5) yielded a minimum crushing roller rotational speed of 1711 r/min.

To ensure the dynamic balance of the blade shaft, two groups of combined blades were symmetrically arranged in the same rotational plane. The combined blades were configured in a double-headed helical pattern along the shaft. Specifically, each helix was equipped with eight combined blades, and each combined blade consisted of five individual blades, resulting in a total of 80 blades. The straw crushing incorporation machine adopted in the experiment had a working width of 1.8 m, with a blade installation density of 44 blades per meter, which satisfied the technical requirements for blade installation density[33].

4 Parameter optimization of crushing roller

Based on parameter design, orthogonal experiments were conducted using the qualification rate of crushing straw and the straw spreading uniformity as evaluation indicators to optimize the blade arrangement, L-shaped blade bending angle, rotational speed, and forward speed of the crushing roller equipped with straight and L-shaped combined blades.

4.1 Experiment conditions and equipment

The experiment was conducted in Putuan Township, Huarong District, Ezhou City, Hubei Province. The tools required for the experiment included a ruler (60 cm), a tape measure (5 m), a sampling frame (500 mm×500 mm), an electronic scale (accuracy of 0.1 g), a circular soil cutter, a TYD-2 soil firmness measuring instrument (±1%), and an electric hot-air drying oven. The average soil firmness at a depth of 10 cm below the soil surface was 653.0 kPa, and the average soil moisture content was 19.2%. At a soil depth of 10-20 cm below the soil surface, the average soil firmness was 2724.2 kPa, and the average soil moisture content was 20.5%. The average stubble height was 61.0 cm, the average straw weight per square meter was 961.6 g, and the average moisture content of the straw was 30.8%.

The experiment was carried out on a straw crushing incorporation machine, which was manufactured by Dinaer Technology Co., Ltd. located in Huarong District, Ezhou City, Hubei Province, China, and its structure is illustrated in Figure 5. One end of the crushing roller is connected to the side plate, while the other end is linked to the output shaft of the gearbox. During operation, the output shaft of the tractor transmitted power to the gearbox, which drove the crushing roller to operate via the pulley after direction reversal and speed adjustment, thereby achieving straw crushing for straw incorporation.

By replacing the blade shaft, the arrangement of the combined blades could be changed. Different L-shaped blades with varying bending angles could be replaced via the blade holders. The rotational speed of the blade shaft could be adjusted by modifying the speed of the tractor's rear PTO (Power Take-Off) shaft. The forward speed of the machine could be adjusted by shifting the forward gear and regulating the throttle.

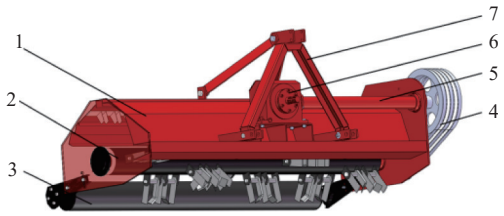

1. Cover shell 2. Crushing roller 3. Press roller 4. Belt wheel 5. Drive shaft 6. Gearbox 7. Three-point suspension device

Figure 5 Experimental device

4.2 Experiment factors and levels

The parameters of the combined blade included blade length, blade thickness, blade width, cutting edge angle, L-shaped blade bending angle, spacing between the five blades in the set, blade arrangement, rotational speed, and forward speed. The blade length of straight blades and L-shaped blades was the difference between the tip radius (240 mm) and the shaft diameters of 90 mm and 150 mm. The width of straight and L-shaped blades was 50 mm, the thickness was 5 mm, and the cutting edge angle was 30°. The spacing between adjacent blades in the combined blades was equal (28 mm each). The axial bending length of the L-shaped blade was 35 mm, so the axial spacing between the central straight blade and the L-shaped bent blade was 28 mm, and the axial spacing between the side straight blades and the L-shaped blade was 73 mm (28 mm + 35 mm). The blades were arranged in a double-helix pattern, determined by two of the three parameters (diameter, helix angle, and pitch), which satisfied:

$$\tan\gamma = \frac{\pi D}{P} \tag{6}$$

During the installation of the combined blade, when viewed axially, each combined blade was evenly distributed around the circumference, and the radial angle between adjacent combined blades was:

$$\alpha = 360/a \tag{7}$$

Helix pitch:

$$P = ab \tag{8}$$

Substituting Equations (7) and (8) into Equation (6) yields the following relationship between the helix angle and the radial angle between adjacent combined blades:

$$\tan\gamma = \frac{\pi D\alpha}{360b} \tag{9}$$

In Equations (6) to (9), γ is the helix angle, (°); D is the blade shaft diameter, mm; P is the helix lead, mm; α is the radial angle between adjacent combined blades, (°); a is the number of combined blades on a single helix; b is the axial installation distance between adjacent combined blades (the distance between the respective symmetrical center axes of the combined blades, equal to the ratio of the working width to the number of combined blades, i.e., 1.8 m/8 = 225 mm).

From Equations (6) and (9), it could be seen that under the conditions where the axial installation distance between adjacent combined blades and the blade shaft diameter were determined, the parameters of the spiral line could be determined by the radial angle between combined blades. Therefore, the radial angle between combined blades was adopted as the characteristic parameter for blade arrangement. To reduce the occurrence of straw congestion, which affected both straw crushing efficiency and straw spreading efficiency, the radial angle should not be designed to be excessively

small[34]. Experiments were conducted with radial angles (Factor A) of 30°, 50°, 70°, and 90°, and the blade arrangements for different radial angles are shown in Figure 6.

According to the reference [35], the L-shaped blade bending angle (Factor B) typically ranges from 100° to 150°; the experimental settings for the L-shaped blade bending angle were: 105°, 120°, 135°, and 150°. The experimental tractor had two speed outputs: 540 r/min and 720 r/min, corresponding to crushing roller rotational speeds (Factor C) of 1800 r/min and 2400 r/min. The tractor used in the experiment was the Dongfanghong LX904 (YTO Group Corporation, Luoyang, Henan Province, China), which had two forward gears: high-speed and low-speed, corresponding to the travel gear and working gear, respectively. Before the experiment, the tractor gear was adjusted to low-speed gear, the throttle was fully depressed, and the forward speeds of the implement (Factor D) were measured as 0.60 m/s and 0.85 m/s. The experiment factor level table is listed in Table 1.

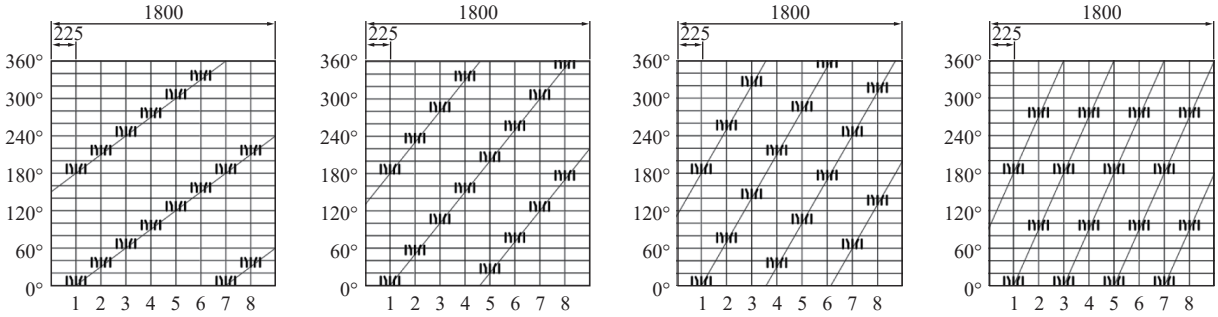

a. Radial angle of 30° b. Radial angle of 50° c. Radial angle of 70° d. Radial angle of 90°

Figure 6 Distribution of combined blades with different radial angle

Table 1 Experimental factors and levels

Levels	Factors			
	Radial angle (A)/(°)	L-shaped blade bending angle (B)/(°)	Rotational speed (C)/ r·min^{-1}	Forward speed (D)/m·s^{-1}
1	30	105	1800	0.60
2	50	120	2400	0.85
3	70	135		
4	90	150		

4.3 Experiment method and measurement index

The experiment adopted a mixed-level orthogonal design with two factors at four levels and two factors at two levels, utilizing an L_{16} ($4^4\times2^3$) orthogonal array, resulting in a total of 16 experimental groups. In each group, the experimental working section length was 30 m. The first and last 5 m of the experimental area were excluded as the data collection area. Within the collection zone, three measurement points were distributed at the ends and the midpoint of a single diagonal line. At each measurement point, the mass of straw with a length of less than 15 cm and the total straw mass within a 0.5 m × 0.5 m area centered on the measurement point was measured. According to China's national standard definition, the qualification rate of straw crushing was calculated using Equation (10), and the straw spreading uniformity was calculated using Equation (11)[36]:

$$\eta = \frac{1}{N}\sum_{1}^{N}\frac{n_i}{m_i}\times 100\% \quad (10)$$

$$u = 1 - \frac{\sqrt{\frac{1}{N-1}\sum_{i=1}^{N}\frac{(m_i-\bar{m})^2}{2}}}{\bar{m}}\times 100\% \quad (11)$$

where, η represents the qualification rate of straw crushing, %; u represents the straw spreading uniformity; m_i is the total mass of straw in the measurement area, g; n_i is the mass of straw with a length less than 15 cm in the measurement area, g; $\bar{m}$ is the average mass of straw (g), $\bar{m} = \frac{1}{N}\sum_{i=1}^{N} m_i$; N is the number of measurement areas, N=3.

4.4 Analysis of experiment results

Based on the measured data and Equations (10) and (11), the qualification rate of straw crushing, the uniformity of straw spreading, and the range of variation for each group of experiments are listed in Table 2.

As shown in Table 2, range analysis indicates that the radial angle and rotational speed had a highly significant impact on the qualification rate of straw crushing, while the L-shaped blade bending angle and forward speed had a significant impact on the qualification rate of straw crushing. The four factors affecting the qualification rate of straw crushing, in descending order of significance, were the radial angle, rotational speed, L-shaped blade bending angle, and forward speed. The radial angle and L-shaped blade bending angle had a highly significant impact on the uniformity of straw spreading, while the rotational speed and forward speed had a significant impact on the uniformity of straw spreading. The factors affecting the uniformity of straw spreading, in descending order of significance, were the radial angle, L-shaped blade bending angle, forward speed, and rotational speed.

4.4.1 Effect of radial angle on experiment results

The analysis of the extreme differences showed the effect of the radial angle (Factor A) on the qualification rate of straw crushing and the uniformity of straw spreading, as shown in Figure 7. The qualification rate of straw crushing first increased and then decreased with an increase in the radial angle. When the radial angle between adjacent moving combination blades is small, it is easy to cause straw blockage, impairing the cutting and crushing efficiency. However, when the radial angle reached 90°, due to the double spiral installation of the combined blades, the angle between the two combination blades in the same rotational plane was 180°, causing the 3rd, 5th, and 7th combination blades on one spiral line to align with the 1st, 3rd, and 5th combination blades on the other spiral line. Additionally, the 1st, 4th, and 8th combination blades on each spiral line aligned with themselves, resulting in a larger number of combined blades cutting the straw simultaneously. This reduced the collision and crushing of straw between different combined blades, which decreased the qualification rate of straw crushing. The

Table 2 Experiment results and analysis

Experiment number		Factors							Results	
		Radial angle (A)/(°)	L-shaped blade bending angle (B)/(°)	Error column	Error column	Rotational speed (C)/r·min^{-1}	Forward speed (D)/r·min^{-1}	Error column	Qualification rate of straw crushing/%	Straw spreading uniformity/%
	1	1(30)	1(105)	1	1	1(1800)	1(0.6)	1	79.54	75.08
	2	1(30)	2(120)	2	2	1(1800)	2(0.85)	2	77.27	72.32
	3	1(30)	3(135)	3	3	2(2400)	1(0.6)	2	86.19	82.53
	4	1(30)	4(150)	4	4	2(2400)	2(0.85)	1	84.05	79.61
	5	2(50)	1(105)	2	3	2(2400)	2(0.85)	1	81.48	84.33
	6	2(50)	2(120)	1	4	2(2400)	1(0.6)	2	84.59	81.04
	7	2(50)	3(135)	4	1	1(1800)	2(0.85)	2	80.32	84.93
	8	2(50)	4(150)	3	2	1(1800)	1(0.6)	1	83.68	87.16
	9	3(70)	1(105)	3	4	1(1800)	2(0.85)	2	86.19	80.4
	10	3(70)	2(120)	4	3	1(1800)	1(0.6)	1	86.47	80.48
	11	3(70)	3(135)	1	2	2(2400)	2(0.85)	1	91.46	83.31
	12	3(70)	4(150)	2	1	2(2400)	1(0.6)	2	90.55	88.19
	13	4(90)	1(105)	4	2	2(2400)	1(0.6)	2	85.51	82.09
	14	4(90)	2(120)	3	1	2(2400)	2(0.85)	1	84.87	78.14
	15	4(90)	3(135)	2	4	1(1800)	1(0.6)	1	86.11	83.62
	16	4(90)	4(150)	1	3	1(1800)	2(0.85)	2	85.01	78.29
Qualification rate of straw crushing	$k1$	81.76	83.18	85.15	83.82	83.07	85.33	84.71		
	$k2$	82.52	83.3	83.85	84.48	86.09	83.83	84.45		
	$k3$	88.67	86.02	85.23	84.79					
	$k4$	85.38	85.82	84.09	85.24					
	R	6.91	2.84	1.38	1.42	3.02	1.5	0.26		
	F-value	26.04**	6.36*	\	\	24.02**	5.94*	\		
	Sequence	$A>C>B>D$ (Radial angle> Rotational speed > L-shaped blade bending angle > Forward speed)								
	Optimal solution	$A_3B_3C_2D_1$								
Straw spreading uniformity	$k1$	77.39	80.48	79.43	81.59	80.29	82.52	81.47		
	$k2$	84.37	78	82.12	81.22	82.41	80.17	81.22		
	$k3$	83.1	83.6	82.06	81.41					
	$k4$	80.54	83.31	81.78	81.17					
	R	6.98	5.6	2.68	0.36	2.12	2.36	0.24		
	F-value	12.99**	9.53**	\	\	6.14*	7.60*	\		
	Sequence	$A>B>D>C$ (Radial angle> L-shaped blade bending angle > Forward speed> Rotational speed)								
	Optimal solution	$A_2B_3C_2D_1$								

Note: A, B, C, and D represent the radial angle, L-shaped blade bending angle, rotational speed, and forward speed, respectively. i denotes the i-th level of the factors; ki represents the arithmetic mean of all experimental result data corresponding to the i-th level in the column for the target factor, which can be used to determine the optimal level and influence intensity of the factor, as well as to calculate the variance. * denotes a significant effect (F0.01>F>F0.05), and ** denotes a highly significant effect (F>F0.01).

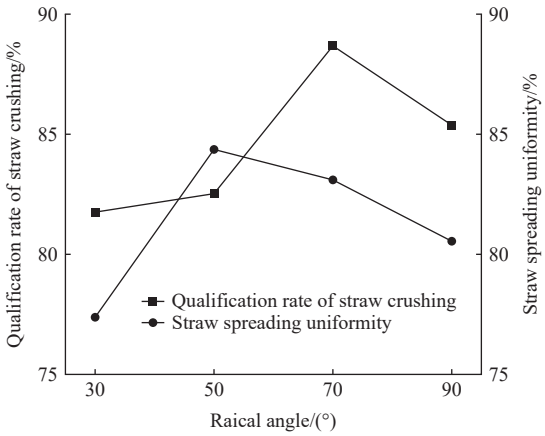

Figure 7 Effect of radial angle on the results

uniformity of straw spreading also followed a pattern of first increasing and then decreasing as the radial angle (Factor A) increased. When the radial angle is too small, blockages and accumulation are more likely to occur, resulting in uneven distribution. When the radial angle between the combined blades was too large, the straw resided for an excessively long time between adjacent combined blades, and some straw fell before reaching the adjacent blades, resulting in reduced straw spreading uniformity.

The radial angle corresponding to the highest qualification rate of straw crushing was 70°, while the radial angle corresponding to the highest straw spreading uniformity was 50°. Since the difference in spreading uniformity between 70° and 50° was only 1.27 percentage points, the optimal radial angle was determined as 70°.

4.4.2 Effect of the L-shaped blade bending angle on the experiment results

The trend of the influence of the L-shaped blade bending angle (B) on the qualification rate of straw crushing is shown in Figure 8. Although when the L-shaped blade bending angle exceeds 135°, the qualification rate of straw crushing decreased slightly (by 0.2 percentage points) as the L-shaped blade bending angle increased, the qualification rate of straw crushing generally exhibited a gradual increasing trend as the L-shaped blade bending angle increased. This is because a larger L-shaped blade bending angle resulted in stronger cutting action and higher crushing efficiency. When the L-shaped blade bending angle (B) exceeded 120°, its impact on straw spreading uniformity followed the same trend as its impact on straw crushing efficiency. On one hand, the increased straw crushing efficiency facilitated uniform straw

distribution. On the other hand, a larger L-shaped blade bending angle increased the contact area between the blade and the straw, enhanced the straw's kinetic energy, and improved the spreading uniformity. Therefore, the optimal L-shaped blade bending angle for the L-shaped blade was determined as 135°.

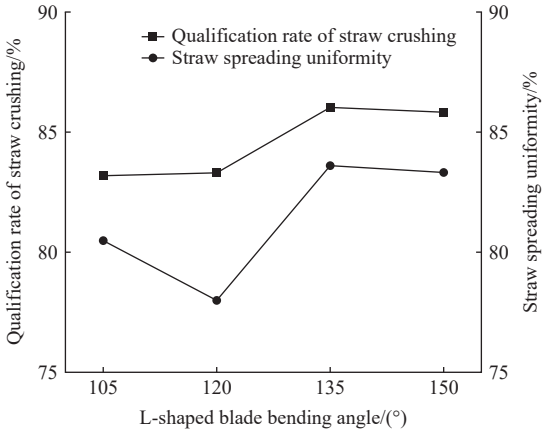

Figure 8 Effect of L-shaped blade bending angle on the results

4.4.3 Effects of rotational speed and forward speed on experiment results

Both the qualification rate of straw crushing and the straw spreading uniformity increased with the increase in the rotational speed. On the one hand, increasing the rotational speed of the crushing roller not only enhanced the cutting line speed of the blades but also increased the frequency with which the blades cut the straw, thereby improving the cutting and crushing effect. On the other hand, the higher the rotational speed, the stronger the negative pressure generated inside the housing, which enhanced the adsorption and pickup effect on the straw, thereby helping to enhance the uniformity of straw spreading. Of course, excessively high rotational speeds could also lead to machine vibrations and a significant increase in power consumption. In this study, an optimized rotational speed of 2400 r/min was determined as the crushing roller. A lower forward speed increased the time the blades interact with the straw during cutting and crushing, thereby increasing the kinetic energy imparted to the straw. This helped improve the qualification rate of straw crushing and spreading uniformity. The optimal forward speed was determined to be the tractor's minimum operating speed of 0.60 m/s.

5 Field experiment of rice straw incorporation machine by crushing-rotary tillage-burying

The optimal operating parameters for the crushing roller were determined through optimization as $A_3B_3C_2D_1$ (where A, B, C, D represent the radial angle, L-shaped blade bending angle, rotational speed, and forward speed, respectively), corresponding to a radial angle of 70°, an L-shaped blade bending angle of 135°, a rotational speed of 2400 r/min, and a forward speed of 0.60 m/s. Field experiments were conducted using these parameters. The validation experiment and parameter optimization experiment were carried out on the same plot of land. The average stubble height was 60.5 cm, the average straw quantity per square meter was 943.5 g, and the average moisture content of the straw was 28.8%. The before-and-after operation effect diagrams are shown in Figure 9. The optimized crushing roller, with straight and L-shaped combined blades, effectively crushed the straw and uniformly spread it over the soil surface.

Using the same measurement method as that in the orthogonal experiment, the qualification rate of straw crushing was found to be 92.41%, and the straw spreading uniformity was 87.44%. A comparison of the optimized experimental results with the orthogonal experimental results is shown in Figure 10.

a. Field experiment process b. Soil surface condition before the work c. Performance of the straw crushing and spreading after the work

Figure 9 Field experiment effect

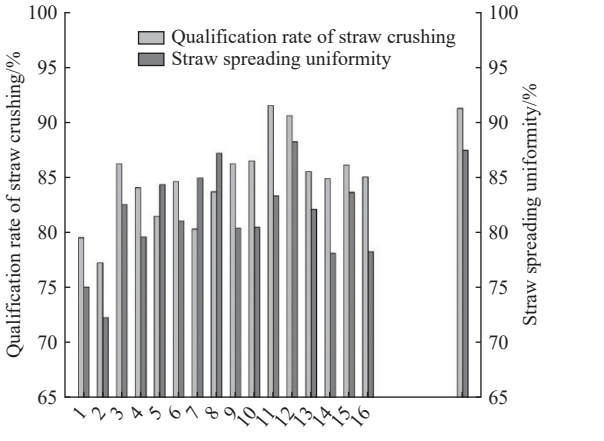

Figure 10 Comparison of results between the orthogonal experiment group and the validation experiment group

As shown in Figure 10, and combined with Table 2, compared to Group 11 with the highest straw crushing qualification rate (91.45%) and the highest spreading uniformity (83.31%) among the 16 groups of orthogonal experiments in the optimized results, the straw crushing qualification rate increased by approximately 1 percentage point, and the spreading uniformity increased by 4.13 percentage points. Compared with Group 12 with the highest spreading uniformity among the 16 orthogonal experiments (straw crushing qualification rate of 90.55%, straw spreading uniformity of 88.19%), the optimized results exhibited an increase of approximately 1.86 percentage points in the straw crushing qualification rate and a difference of only 0.75 percentage points in straw spreading uniformity.

As shown in Table 3, compared with China's national standard requirements, the optimized results showed a 2.41 percentage point increase in straw crushing qualification rate and a 12.44 percentage

point increase in straw spreading uniformity, thus meeting and exceeding China's national standards. The straw crushing qualification rate and spreading uniformity of the optimized combined blades were better than those of other combined blade types.

Table 3 Comparison of experimental results

Combined blade types	Average length of crushed straw/cm	Qualification rate of straw crushing/%	Straw spreading uniformity/%	Source
Three straight blades + two L-shaped blades	10.54	92.41	87.44	This paper
A straight blade + two L-shaped blades	11.00	91.47	\	[27]
A cross straight blade + two L-shaped blades	\	90.01	77.45	[28]
National standard of China	≤15	90	75	[34]

6 Conclusions

To enhance the crushing degree and spreading uniformity of high-stubble, high-density rice straw for straw incorporation, a crushing roller equipped with combined straight and L-shaped blades was designed. Parametric optimization and experimental validation were carried out on this crushing roller. Taking radial angle, L-shaped blade bending angle, rotational speed, and forward speed as experimental factors, and with qualification rate of straw crushing and straw spreading uniformity as measurement indicators, a mixed-level orthogonal experiment (two factors at four levels and two factors at two levels) was conducted. The research conclusions are as follows:

(1) The results indicated that the factors influencing the straw crushing qualification rate, in descending order of significance, were the radial angle, rotational speed, L-shaped blade bending angle, and forward speed. For straw spreading uniformity, the influencing factors in descending order of significance were the radial angle, L-shaped blade bending angle, forward speed, and rotational speed. The optimal parameter combination was determined to be a radial angle of 70°, an L-shaped blade bending angle of 135°, a rotational speed of 2400 r/min, and a forward speed of 0.60 m/s.

(2) The results of the validation experiment showed that under the optimal parameter combination, the straw crushing qualification rate reached 92.41% and the straw spreading uniformity was 87.44%. Compared with the control group, the straw crushing qualification rate increased by approximately 1.86 percentage points, and the straw spreading uniformity differed by only 0.75 percentage points from the maximum value recorded in the orthogonal experiments, thus meeting and exceeding the requirements of China's national standards. The straw crushing qualification rate and spreading uniformity of the optimized combined blades were superior to those of other combined blade types.

Acknowledgement

This work was supported by the National Natural Science Foundation of China (Grant No. 52175233).

[References]

[1] National Bureau of Statistics of the People's Republic of China. China Statistical Yearbook. Beijing: China Statistics Press, 2024. (in Chinese)

[2] Shu Y, Liu Y X, Liu M M, Bi J. Energy potential and bioethanol production potential from collectable major crop residue in China. Journal of Beijing Institute of Technology (Social Science Edition), 2023; 25(5): 64–72.

[3] Cuong O Q, Demont M, Pabuayon I M, Depositario D P T. What drives rice farmers away from straw burning? Evidence from the Mekong Delta, Vietnam. Environmental Challenges, 2025; 19: 101150.

[4] Mahmoud M A M, Said A E A A, Elhafeez H H A, Soliman S A, Mahmoud U T. Maize stover burning exposure accountable for remarkable environmental and health risk in broiler chickens. BMC Veterinary Research, 2025; 21(1): 199–199.

[5] Sun G F, Sun R H, Zhou W, Liu J H, Sheng J, Xu Z Y. Effects of long-term straw returning on rice yield and surface water environment. China Rice, 2023; 29(5): 57–61.

[6] Wang Z Y, Chen W H, Yuan W, Zhou Z P. Effects of long-term straw returning and tillage ways on yield and quality of rice. China Rice, 2021; 27(3): 17–20, 29.

[7] Sun C M, Dong Y B, Ji L, Chen C, Zhang A K, Zhong P. Technology of agricultural utilization of plant ash, the waste of biomass power plants. Barley and Cereal Science, 2022; 39(06): 60–66, 70.

[8] Liang C B, Li J G, Shen F, Liu B, Han Y, Yao J P. Effect of transplanting density and biochar application on the yield of rice. China Soil and Fertilizer, 2021; 2: 240–247.

[9] Latifmanesh H, Deng A X, Li L, Chen Z J, Zheng Y T. How incorporation depth of corn straw affects straw decomposition rate and C&N release in the wheat-corn cropping system. Agriculture, Ecosystems and Environment, 2020, 300. DOI: 10.1016/j.agee.2020.107000

[10] Negiş H, Şeker C. Effects of maize and sunflower straws with chemical fertilizer in corporations on nutrient contents of the soil and the yield components of maize plant. Journal of Plant Nutrition, 2025; 48(9): 1455–1471.

[11] Yang X Y. Analysis of the decomposition rate of rape straw decay under three modes. Southern Agriculture, 2014; 8(22): 40–41.

[12] Pang L D. Decomposition rate of corn straw returning and its effects on soil nutrients. Harbin: Northeast Agricultural University, 2017. DOI: 10.7666/d.Y3231384. (in Chinese)

[13] Hu H X, Cheng Y, Ma Y H, Yu X S, Xiang J X. Decomposition characteristics of returned rapeseed straw in soil and effects on soil fertility. Chinese Journal of Eco-Agriculture, 2012; 20(3): 297–302.

[14] Qin K, Cao C M, Liao Y S, Wang C Q, Fang L F, Ge J. Design and optimization of crushing and throwing device for straw returning to field and fertilizing hill-seeding machine. Transactions of the CSAE, 2020; 36(3): 1–10.

[15] Tian Z H, Gao S M, Zhu E, Zhang C H. Effect of non uniform returning of wheat straw to field on growth of direct sown rice and countermeasures concerned. Soil and Fertilizer Sciences in China, 2002; 1: 26–29.

[16] Liang F, Luo L Q, Zhan S P, Wang J K, Gu J W, Shu X. Effects of the length and spatial distribution of rapeseed straw returning field on corn sowing quality. Transactions of the CSAE, 2025; 41(5): 50–56.

[17] Shi Y Y, Luo W W, Hu Z C, Wu F, Gu F W, Chen Y Q. Design and experiment of equipment for straw crushing with strip-laying and seed-belt classification with cleaning under full straw mulching. Transactions of the CSAM, 2019; 50(4): 58–67.

[18] Sun N N, Wang X Y, Li H W, He J, Wang Q J, Wang J, et al. Design and experiment of differential sawing rice straw chopper for turning to field. Transactions of the CSAE, 2019; 35(22): 267–276.

[19] Liu D, Wang X Y, Li H W, He J, Wang Q J. Design and experiment of active centrifugal rice straw spreading device. Transactions of the CSAM, 2024; 55(S1): 81–91.

[20] Lin H, He J, Li H, Wang C, Li H, Tan L. Design and experiment of variable-speed straw chopping machine based on PLC control with equal diameter cam transmission. Transactions of the CSAM, 2024; 55(7): 96–110.

[21] Yan L M, Wu T, Jiang D L, Gou H X, Fu X H, Zhang J H. Design and experiment of side-throwing cotton stalk crushing and returning device. Transactions of the CSAM, 2025; 56(3): 216–226.

[22] Ergashev I T, Islamov Y I, Pardayev X Q, Tashtemirov B R, Ismatov A I, Abdullaev B V. Results of the research of a combined aggregate straw grinder, which sows seeds of repeated crops. IOP Conference Series: Earth and Environmental Science, 2021; 868(1): 12087.

[23] Masienko I, Fedulenko D, Tatarintsev V. Development prospects of mobile rice straw crushers. E3S Web of Conferences, 2019; 12600022. DOI: 10.1051/e3sconf/201912600022

[24] Zhang H M, Chen X G, Yan L M, Yang S M. Design and experiment of master-slave straw returning and residual film recycling combine machine.

Transactions of the CSAE, 2019; 35(19): 11–19.

[25] Shi Y Y, Wang X C, Hu Z C, Gu F W, Wu F, Chen Y Q. Optimization and experiment on key structural parameters of no-tillage planter with straw-smashing and strip-mulching. Int J Agric & Biol Eng, 2021; 14(3): 103–111.

[26] Liu X L, Zhao W Y, Zhang H, Wang G P, Sun W, Dai F, et al. Design and experiment of an upper-side-discharge straw-returning and bundle self-unloading integrated corn residual film recycling machine. Int J Agric & Biol Eng, 2023; 16(5): 61–70.

[27] Jia H L, Jiang X M, Guo M Z, Liu X L, Wang L C. Design and experiment of V-L shaped smashed straw blade. Transactions of the CSAE, 2015; 31(1): 28–33.

[28] Zhang X R, Ni S L, Liu J X, Hu X H, Zhang Z F, Fu S H. Design and flow field analysis of bionic blade of banana straw crushing and throwing machine. Transactions of the CSAM, 2024; 55(8): 138–151, 160.

[29] Luo W W, Gu F W, Wu F, Xu H B, Chen Y Q, Hu Z C. Design and experiment of wheat planter with straw crushing and inter-furrow collecting-mulching under full amount of straw and root stubble cropland. Transactions of the CSAM, 2019; 50(12): 42–52.

[30] Zhang Z Q, He J, Li H W, Wang Q J, Ju J W, Yan X L. Design and experiment on straw chopper cum spreader with adjustable spreading device. Transactions of the CSAM, 2017; 48(9): 76–87.

[31] Singh A, Dhaliwal I, Dixit A. Performance evaluation of tractor mounted straw chopper cum spreader for paddy straw management. Indian Journal of Agricultural Research, 2011; 45(1): 21–29.

[32] Fan G Q, Wang Z Y, Wang B X, Wang J X, Dong H Y, Han J. Design and experiment of rotary feed tube hammer grinder. Transactions of the CSAM, 2021; 52(12): 43–53, 76.

[33] Wei S Q, Li Y, Wu Z H, Li Z Q. Optimization design of key components of horizontal banana straw crushing and returning machine. Journal of Agricultural Mechanization Research, 2024; 46(12): 58–66.

[34] Wang Y Q, Deng Y G, Chen P M, Yan B. Design and research on anti-entanglement weed shredder. Journal of Agricultural Mechanization Research, 2025; 47(10): 107–114.

[35] Liu P, He J, Li Y J, Li H W, Wang Q J, Lu C Y, et al. Design and experiment of double rollers maize stalk chopping device with different rotation speeds. Transactions of the CSAE, 2020; 36(14): 69–79.

[36] National Technical Committee for the Standardization of Agricultural Machinery (SAC/TC 201). Conservation tillage equipment-part 6: smashed straw machine: GB/T 24675.6-2021. China Standard Press, 2021. (in Chinese)